

Article

# (1S,2S)-Cyclohexane-1,2-diamine-based Organosilane Fibres as a Powerful Tool Against Pathogenic Bacteria

Veronika Mátková <sup>1,\*</sup>, Barbora Holubová <sup>1</sup>, David Tetour <sup>2</sup>, Jiří Brus <sup>3</sup> , Michal Řezanka <sup>1</sup> ,  
Miroslava Rysová <sup>4</sup> and Jana Hodačová <sup>2</sup> 

<sup>1</sup> Department of Nanomaterials in Natural Science, Institute for Nanomaterials, Advanced Technologies and Innovation, Technical University of Liberec, Studentská 1402/2, 461 17 Liberec, Czech Republic; barbora.holubova@tul.cz (B.H.); michal.rezanka@tul.cz (M.Ř.)

<sup>2</sup> Department of Organic Chemistry, University of Chemistry and Technology, Prague, Technická 5, 166 28 Prague, Czech Republic; davidtetour@seznam.cz (D.T.); jana.hodacova@vscht.cz (J.H.)

<sup>3</sup> Institute of Macromolecular Chemistry, Academy of Sciences of the Czech Republic, Heyrovsky Sq. 2, 162 06 Prague, Czech Republic; brus@imc.cas.cz

<sup>4</sup> Department of Nanomaterials and Informatics, Institute for Nanomaterials, Advanced Technologies and Innovation, Technical University of Liberec, Studentská 1402/2, 461 17 Liberec, Czech Republic; miroslava.rysova@tul.cz

\* Correspondence: veronika.makova@tul.cz; Tel.: +420-485-353-863

Received: 14 December 2019; Accepted: 12 January 2020; Published: 14 January 2020



**Abstract:** An urgent need to find an effective solution to bacterial resistance is pushing worldwide research for highly effective means against this threat. Newly prepared hybrid organosilane fibres consisting of a (1S,2S)-cyclohexane-1,2-diamine derivative, interconnected in the fibre network via covalent bonds, were fully characterised via different techniques, including FTIR, TGA-FTIR, SEM-EDS, and solid-state NMR. Fibrous samples were successfully tested against two types of pathogenic bacterial strains, namely *Staphylococcus aureus*, and *Pseudomonas aeruginosa*. The obtained results, showing >99.9% inhibition against *Staphylococcus aureus* and *Pseudomonas aeruginosa* in direct contact compared to the control, may help particularly in case of infections, where there is an urgent need to treat the infection in direct contact. From this point of view, the above-mentioned fibrous material may find application in wound healing. Moreover, this new material has a positive impact on fibroblasts viability.

**Keywords:** organic-inorganic hybrids; organo-bridged silsesquioxane; sol-gel process; electrospinning; *Staphylococcus aureus*; *Pseudomonas aeruginosa*

## 1. Introduction

Pathogenic bacteria have become a worldwide problem. According to the World Health Organization (WHO) statistics, over 1.4 million people worldwide suffer from infections caused by pathogenic bacteria acquired in hospitals [1]. *Staphylococcus aureus* (*S. aureus*) and *Pseudomonas aeruginosa* (*P. aeruginosa*) are among the most problematic pathogenic bacteria closely connected with an extremely overgrowing resistance to antibiotics, which brings another major complication in the treatment [2,3]. The infections caused by *P. aeruginosa* are usually resistant to multiple antibiotics due to the bacterium's intrinsic resistance [4]. It is important to note that both bacterial strains are 1000 times more resistant in the form of a biofilm [5].

Due to the antibiotic resistance of these bacteria, great effort has been devoted to developing new antibiotics. One group of such compounds are, for example, *trans*-cyclohexane-1,2-diamine derivatives (DACHs). Previous studies have proved them to be very promising antibacterial compounds against *P.*

*aeruginosa* [6], *Mycobacterium tuberculosis* [7–9], and *S. aureus* [6,8]. Moreover, it was found that (1*S*,2*S*) enantiomers generally have lower minimum inhibitory concentrations compared to racemate [6].

Functional organosilica or organosilane-based hybrids for biomedicine applications are well known to the academic public and in various industrial applications [10–14]. In general, an ever-growing interest [13] lies not only in the mild synthesis conditions offered by the sol-gel process producing a broad range of end-products but also in the possibility of nanoscale tailoring of their chemical structure fulfilling the specific needs of biocompatibility and mechanical properties of targeted bio-applications [10–16].

Organosilica and organosilane materials with antibacterial properties are found particularly in the form of nanoparticles [17] or thin coatings [18] on various substrates. Surprisingly, the preparation of the hybrid fibres based on bridged organo-bis-silylated precursors is rarely reported [19,20]. Furthermore, in most cases, hybrid fibres are produced as a combination of silica alkoxides or organo-mono-silylated precursors mixed with organic polymers (poly( $\epsilon$ -caprolactone)/polyethylene terephthalate/polyvinylalcohol etc.) or biopolymers [16,18,21,22]. However, such materials are less degradable, and often inappropriate solvents, or precursors are employed. An example of such material is polyhydroxybutyrate/poly( $\epsilon$ -caprolactone)/silica hybrid nanofibrous scaffolds for bone tissue regeneration [23,24] or electrospun organosilane-loaded collagen nanofibrous scaffolds containing quaternary ammonium organosilane and octadecyldimethyl(3-trimethoxysilylpropyl)ammonium chloride with antibacterial activity [25].

To the best of our knowledge, a fibrous system combining the advantages of organosilane and cyclohexane-1,2-diamine derivatives has not been studied yet (or even prepared). This system may offer an answer to the urgent need for the development of new types of biomaterials, which may help to improve the problem of difficult-to-heal infections (wounds) caused by pathogenic bacteria in direct contact. This project deals with challenges in the preparation of antibacterial fibres with a pure organosilane composition based on a silylated (1*S*,2*S*)-cyclohexane-1,2-diamine precursor. No surfactants, low-molecular-weight polymeric gelators, or spinnable polymers were used during the subsequent electrospinning process, and the whole one-pot synthesis is based on a one solvent solution to minimise the toxicity of the formation of the fibres and their subsequent use.

## 2. Materials and Methods

Tetraethyl orthosilicate—TEOS (>99%, Merck, Prague Czech Republic), ethanol—EtOH (99.9%, Penta, Prague, Czech Republic), hydrochloric acid (35%, Prague, Czech Republic), deionised water (Milli-Q, Prague, Czech Republic). Aluminium foil thickness 12  $\mu$ m (Rotilabo, Karlsruhe, Germany). (1*S*,2*S*)-1,2-Bis{*N*'-[3-(triethoxysilyl)propyl]ureido}cyclohexane (compound 1) was prepared according to the literature [26].

The standard procedure for the synthesis of a spinnable organosilane sol solution was as follows: Silica precursor composed of TEOS:compound 1 (in a molar ratio of 57:43), ethanol, deionised water, and HCl were added into a round bottom flask and stirred at 450 rpm/r.t./30 min (Table 1). The pH of the sols was adjusted to 2. Finally, the solution was heated to 90 °C in an oil bath at 450 rpm, refluxed for 4 h, and subsequently partially evaporated. The dynamic viscosity was measured before the electrospinning and appropriately adjusted. Hybrid fibres (marked as DACHsilane) were prepared via jet needle electrospinning (Table 1) and finally dried for 24 h in a desiccator for further use.

**Table 1.** Sols tested in electrospinning and conditions employed for the jet needle-electrospinning.

Sol-Gel Parameters			Parameters of Needle-Electrospinning			
Molar Ratio $r =$ [H <sub>2</sub> O]/[silanes]	Molar Ratio Alc = [EtOH]/[silanes]	Viscosity [mPa·s]	Feeding Rate [mL·h <sup>-1</sup> ]	Tip-To-Collector Distance [cm]	High Voltage [kV]	Temperature/Relative Humidity
2.0	9.7	40–60	0.5–1	15–20	20–25	25 °C/30%

Inorganic silica dioxide nanofibres with an average diameter of  $0.33 \pm 0.08 \mu\text{m}$ , prepared according to the already-published procedure [27], were used as a standard material to assess antibacterial and cytotoxicity activity.

## 2.1. Characterisation Techniques

### 2.1.1. Scanning Electron Microscopy

The morphology of the hybrid DACHsilane fibres was studied by SEM (ZEISS Ultra Plus, Sigma Family, Jena, Germany). Samples were sputtered with a 2-nm platinum layer and were subsequently viewed as secondary electron images (1 kV). The fibre diameter was characterised using the NIS Elements software (LIM s.r.o., Liberec, Czech Republic) and was assessed from a total amount of 100 measurements per material, taken from five independent images. The results were evaluated in the form of the mean  $\pm$  standard deviation.

Energy-dispersive X-ray spectroscopy (SEM-EDS, Oxford X-MAX 20, ZEISS Ultra Plus, Sigma Family, Jena, Germany) was used at 10 keV to evaluate the chemical composition of the prepared fibrous (DACHsilane) samples.

### 2.1.2. Fourier Transform Infrared Spectroscopy (FTIR)

FTIR spectrometry was used to assess the chemical structure of the prepared hybrid DACHsilane fibres. FTIR Spectrometer Nicolet iZ10 (Thermo Fisher Scientific, Waltham, MA, USA) with an attenuated total reflection (ATR) diamond crystal angle of  $45^\circ$ , and a spectral range of  $4000\text{--}700 \text{ cm}^{-1}$  was used for the analysis. The number of sample scans: 16, number of background scans: 32, resolution:  $4 \text{ cm}^{-1}$ , gain: 4.0, apodisation: Happ–Genzel, correction: Atmospheric suppression, baseline.

### 2.1.3. $^{29}\text{Si}$ cross Polarization Magic Angle Spinning Nuclear Magnetic Resonance (CP/MAS NMR) Spectroscopy

Solid state NMR analysis was used to evaluate the chemical structure of the prepared DACHsilane fibres. Spectra were measured at 11.7 T using a Bruker AVANCE III HD WB/US NMR spectrometer (Bruker, Ettlingen, Germany) in a double-resonance 4-mm probe head at spinning frequencies  $\omega_r/2\pi = 7$  and 10 kHz. In all cases, finely powdered dry samples were placed into 4-mm  $\text{ZrO}_2$  rotors. All of the experiments were conducted at 303 K. The  $^{29}\text{Si}$  CP/MAS NMR spectra were recorded at Magic Angle Spinning (MAS) of 7 kHz. The spectra were referenced to the external standard M8Q8 ( $-109.8 \text{ ppm}$ ). The number of scans was 0.5–5k depending on the amount of sample. For the quantitative analysis and deconvolution of  $^{29}\text{Si}$  CP/MAS NMR spectra, the TopSpin 3.6 program package (Bruker) was used [28].

### 2.1.4. Thermogravimetric Analysis Fourier Transform Infrared Spectroscopy (TGA-FTIR)

The samples were analysed using a Q500 thermogravimetric analyser (TA Instruments, New Castle, PA, USA). Each sample was placed on a platinum pan and analysed in a non-reactive atmosphere of nitrogen with a flow rate of 60 mL/min. The samples were heated at  $10^\circ\text{C}/\text{min}$ ; the range was from  $20^\circ\text{C}$  to  $650^\circ\text{C}$ . The thermal decompose products were analysed by the Nicolet iS10 FTIR spectrometer (Thermo Fisher Scientific, Waltham, MA USA). Spectra were taken every 10 s with a resolution of  $2 \text{ cm}^{-1}$  in the spectral range of  $4000\text{--}650 \text{ cm}^{-1}$ .

## 2.2. Antibacterial Activity Assessments

All of the tested fibrous samples (round shape, the diameter 0.6 cm) were sterilised for 1 h at  $120^\circ\text{C}$  before each bacterial experiment separately. Pure silica dioxide ( $\text{SiO}_2$ ) fibres were used as standard comparison material in all experiments.

Antibacterial tests were performed using Gram-positive *Staphylococcus aureus* (CCM 3953) and Gram-negative *Pseudomonas aeruginosa* (CCM 3955) (ALE-G18, CSNI, collection of microorganisms,

Masaryk University, Brno, Czech Republic). A Luria–Bertani (LB) broth medium was used to prepare the agar plates (Sigma-Aldrich, Merck, Czech Republic).

### 2.2.1. Qualitative Method

The Kirby–Bauer test was used to analyse the ability of both types of fibres (pure inorganic SiO<sub>2</sub> and hybrid DACHsilane) to inhibit the growth of *S. aureus* and *P. aeruginosa*. A total of 1 mL of both the bacterial inocula (initial optical cell density at 600 nm  $0.15 \pm 0.08$  (McFarland standard concentration =  $0.9 \times 10^7$  CFU/mL)), was spread over four LB agar plates separately using sterile swabs. The samples (round shape, the diameter 0.6 cm) were placed in the centre of the agar plate and incubated for 24 h at 37 °C. The bacterial growth-inhibiting effect was determined by the size of the inhibition zone around the samples.

### 2.2.2. Quantitative Method

The colony-forming unit (CFU) counting method was used to evaluate the antibacterial activities of the pure inorganic SiO<sub>2</sub> fibres (used as a standard comparison material) and newly prepared hybrid DACHsilane fibres against *S. aureus* and *P. aeruginosa* following the reported protocol [29].

The overnight cultures of bacteria (50 mL) in the Luria–Bertani (LB) broth were centrifuged for 5 min at 3780 rcf (relative centrifugal force) to remove supernatant, washed with phosphate-buffered saline (PBS) twice and then re-suspended in a sterile physiological saline solution (0.15 M NaCl, pH 7.0, 20 mM NaHCO<sub>3</sub>) to an initial optical cell density at 600 nm (OD<sub>600</sub>) of  $0.15 \pm 0.08$  (McFarland standard concentration =  $0.9 \times 10^7$  CFU/mL).

Fibrous samples with an approximate diameter of 0.6 mm were placed in sterile Fisher bottles (100 mL) with 20 mL of the prepared bacteria solution separately and were incubated for 5 h at 37 °C. Subsequently, the samples were taken out of the bacteria solution, put into sterile glass vials with 10 mL of physiological saline solution, and were gently shaken in a shaker (Heidolph Unimax 1010, Thermo Fisher Scientific, Pardubice, Czech Republic) for 7 min at 25 °C to remove the attached bacteria. The obtained suspensions were diluted 100 times, and 100 µL of each bacterial solution was taken to plate on (LB) agar plates. Each test was performed in triplicate. Viable colonies of microbes on the agar plate were counted, and the percentage of cell growth reduction (CGR, %) was calculated using the equation  $CGR = (C_0 - C/C_0) \times 100\%$ , where  $C_0$  is the number of CFU of bacteria from the control sample and  $C$  is the number of CFU of bacteria from hybrid DACHsilane fibres [1,29].

### 2.2.3. Bacterial Adhesion

The bacterial adhesion of *S. aureus* and *P. aeruginosa* on the surface of each fibrous sample was evaluated according to the reported literature [29]. Several changes, appearing during the experiment, are mentioned below. The prepared samples were incubated in the bacterial solutions at the initial optical cell density ( $0.15 \pm 0.08/600$  nm) for 1 h at 37 °C. Subsequently, the samples were rinsed twice with distilled water, put on glass slides and covered with a Live/Dead Backlight, 1 Kit 30× diluted solution containing (1.67 mM of SYTO9—A and 18.3 mM propidium iodide—B, molar ratio 1:1). The samples were kept in the dark for 15 min and further analysed at 630 nm using the filters 44 fluorescein isothiocyanate (FITC) (green) and 43 cy3 (red). The live and dead bacteria (*S. aureus* and *P. aeruginosa*) attached to the surface of the samples were imaged using a fluorescent microscope (ZEISS Axio Imager 2, Jena, Germany).

## 2.3. Cytotoxicity Experiments

Cytocompatibility of the DACHsilane hybrid fibres was assessed using murine fibroblasts 3T3-A31. Prior to testing, the cells were maintained in a completed DMEM medium (4.5 g/L D-glucose, L-glutamine, sodium pyruvate, Sigma-Aldrich-Merck, CZ) supplemented with 5% foetal bovine serum (FBS, Biosera, CZ), 5% new-born calf serum (NBCS, Sigma-Aldrich-Merck, CZ), and a 1% penicillin-streptomycin (PS) antibiotic mixture. The cell viability assay was performed in compliance

with the ISO 10993-5:2009 standard with minor modifications. Briefly, the 3T3-A31 fibroblasts were seeded into a 96-well plate (10,000 cells per well) and cultured for 24 h prior to the main experiment. The UV-C sterilised samples were extracted in a supplement-free media for 24 h (37 °C/100 rpm). After the extraction period, macroscopic residues were removed by sterile filtration. The obtained filtrates were supplemented by 5% FBS/5% NBCS/1% PS to final concentrations corresponding to 500 µg, 250 µg, and 125 µg fibres per 1 mL of complete medium. The cells were exposed to 100 µL of these extracts per well for 24 h under standard conditions (37 °C/5% CO<sub>2</sub>). Each sample was tested six times and compared to the cell control (pristine complete medium), positive control (0.1% Triton x-100), and negative control (0.01% L-arginine). The inorganic silica dioxide nanofibres were used as a secondary control and went through the same elution process described above. After exposure for 24 h, the 3-(4,5-dimethyl-2-thiazolyl)-2,5-diphenyl-2H-tetrazolium bromide (MTT, Sigma-Aldrich-Merck, Prague, Czech Republic) viability assay was performed and evaluated by an absorbance reading at 570 nm. The final viability was calculated as a proportion of the cell control value. The results of the cell viability assay were supported by cell morphology evaluation, as described in Figure S6 in the Supplement.

### 3. Results and Discussion

A novel hybrid fibrous material marked as DACHsilane was prepared via electrospinning (Figure 1). Bis-silane precursors are known to behave as network builders during polymerisation and, hence, the resulting fibrous structures display unique material properties. The incorporation of compound 1 then leads to the formation of a hybrid material. This results in a rather weakly-branched, extended polysiloxane matrix required for the fibre-making process [20,30–32].

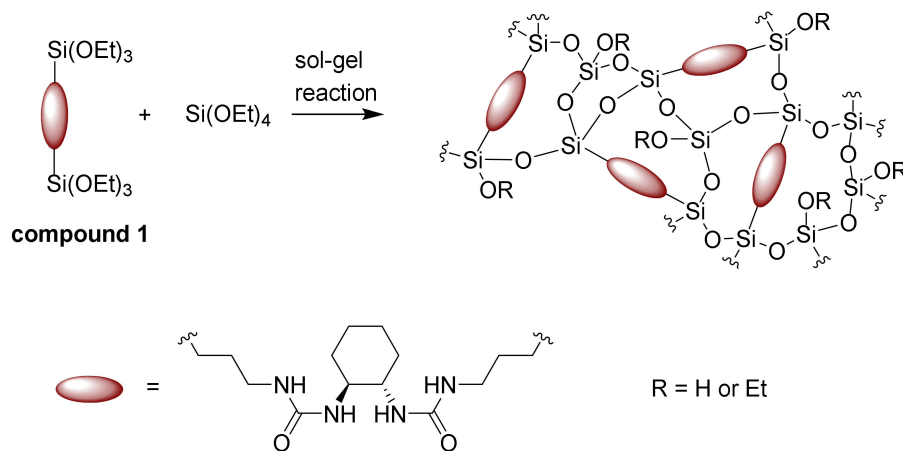


**Figure 1.** The sol-gel process of forming pure hybrid organosilane fibres based on compound 1.

#### 3.1. Characterisation of Pure Organosilane Fibres with DACH Functionality

Morphologically compact and homogeneous fibres with a diameter of  $2.47 \pm 0.91 \mu\text{m}$  (Figure 2a) were obtained via the needle electrospinning method. The prepared organosilane fibres are flexible and do not break during sample manipulation. Some of the fibres have a tendency to form in the helical structure, probably during the electrospinning procedure (inset image in Figure 2a).



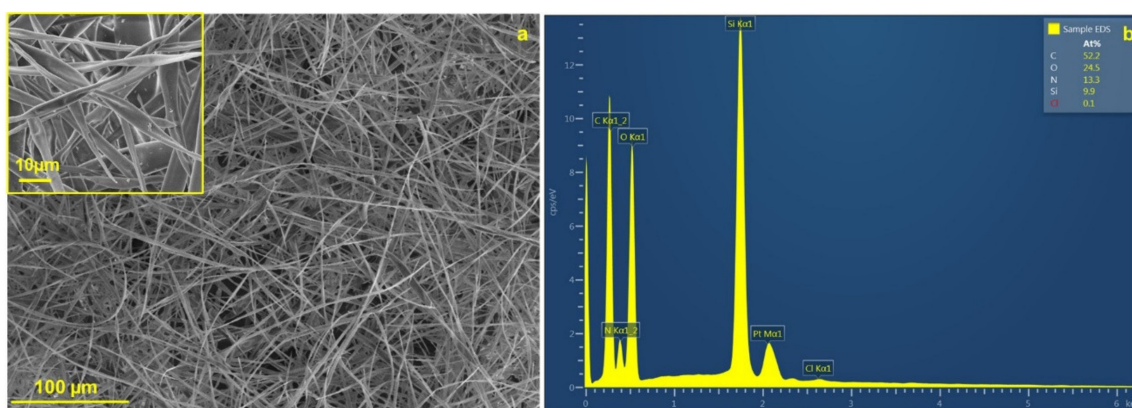


**Figure 2.** SEM image of the prepared hybrid fibres with an inset showing the helical structure of the parts of the fibres (a); Energy Dispersive X-Ray Spectroscopy (EDS) spectra of the hybrid fibres (b).

EDS analysis confirmed the presence of oxygen, carbon, nitrogen, and silicon in the fibrous structure (see Figure 2b). The visibility of nitrogen in the spectra is attributed to the urea functional groups. Moreover, this observation is in compliance with the FTIR result (Figure 3), which confirms the appearance of the characteristic vibrations corresponding to the urea NH-CO-NH and cyclic aliphatic hydrocarbon functionalities in the fingerprint area from  $1700$  to  $1200$   $\text{cm}^{-1}$  (various stretching and bending vibrations). Primarily, the doublet at around  $1630$  and  $1560$   $\text{cm}^{-1}$  (urea units;  $\nu(\text{CO})$  and  $\delta(\text{NH})$ ) and the less intense peak at  $1450$   $\text{cm}^{-1}$  (cyclic aliphatic hydrocarbon unit,  $\delta(\text{CH}_2)$ ) provide strong evidence [33–35] that compound **1** is successfully preserved in the prepared organosilane fibrous material. Moreover, the area from  $1200$  to  $400$   $\text{cm}^{-1}$  proves that no Si–C cleavage occurred in greater amounts, and the silica units progressed well towards the interconnected polysiloxane Si–O–Si network [33,36].

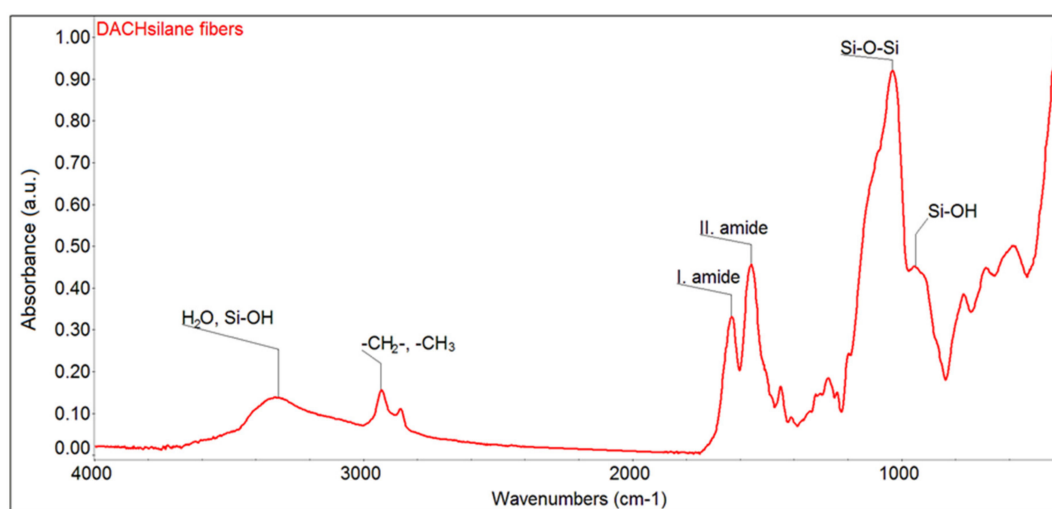


**Figure 3.** FTIR spectra of the prepared hybrid DACHsilane fibres made of compound **1**.

Spectroscopic  $^{29}\text{Si}$  CP/MAS NMR examinations further confirm the correct setting of sol-gel processing parameters in accordance with the above-mentioned research on the sol-gel processing of silica fibres [20,31,32]. The recorded  $^{29}\text{Si}$  CP/MAS NMR spectrum of the studied organosilane mat (Figure 4) exhibits five clearly resolved resonances corresponding to the characteristic structure units of the siloxane network at different condensation reaction rates: two well-pronounced  $T^n$  signals (the organosilane bridged precursor;  $\text{C-Si}(\text{OSi})_n(\text{OH})_{3-n}$ ) and three  $Q^n$  signals (the polysiloxane TEOS matrix;  $\text{Si}(\text{OSi})_n(\text{OH})_{4-n}$ ) [31,33,34]. The overall composition of the siloxane fractions (Table 2) is dominated by incompletely condensed  $T^2$ ,  $Q^2$ , and  $Q^3$  species together with a completely polymerised

T<sup>3</sup> unit. These findings most probably indicate the formation of a ladder-like structure leading to a spinnable linear polymer (Figure 1), as fully-grown 3D Q<sup>4</sup> species would be rather unsuitable for electrospinning. As the organosilane (1) silicon prevails (compound 1:tetraethoxysilane (TEOS) = 43:57 mol.%) in the composition formula, the T<sup>n</sup> signals also dominate in the spectrum. The effect of the hydrolysis-polycondensation reaction inevitably leads to the copolymerisation between the structural units of TEOS and the organosilane modifier [31,37]. Hence, the successful formation of a Class II hybrid material [10] may be confirmed.

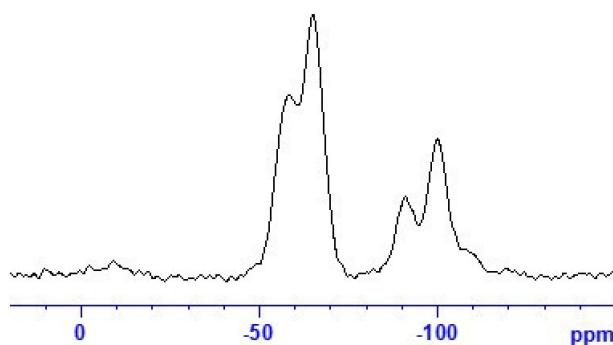


Figure 4. <sup>29</sup>Si CP/MAS NMR spectra of the hybrid DACHsilane fibres.

Table 2. Composition of the siloxane fraction defined as the total amount of individual T<sup>n</sup> and Q<sup>n</sup> structure units in molar %.

Relative Amount of Building Units, %							RATIO Σ
T <sup>1</sup>	T <sup>2</sup>	T <sup>3</sup>	Q <sup>1</sup>	Q <sup>2</sup>	Q <sup>3</sup>	Q <sup>4</sup>	T <sup>n</sup> :Q <sup>n</sup>
1	27	38	0	11	20	3	66:34

The thermogravimetric analysis coupled with FTIR spectroscopy (Figure S1) indicates that the prepared fibrous organosilane material is stable up to 200 °C, where a major weight loss begins and reaches a maximum at around 260 °C. This loss is attributed to the decomposition of the urea unit within the hybrid organosilane network. The TGA-FTIR analysis also confirms the presence of a small portion of water or solvent contained in the fibrous mat most probably originating from incomplete hydrolysis-polycondensation, as previously indicated in the <sup>29</sup>Si CP/MAS NMR spectroscopic evaluation.

### 3.2. Biomedical Applications

#### 3.2.1. Assessment of the Inhibition Zone—Antibacterial Activity in Direct Contact

A qualitative test was performed to evaluate the antibacterial activity of the prepared hybrid DACHsilane fibres in direct contact (Figure S2). The prepared hybrid fibres exhibited a significant antibacterial effect, particularly against *S. aureus* in direct contact (Figure S2b in detail), rather than in the case of *P. aeruginosa*. Standard material, pure SiO<sub>2</sub> fibres, showed no antibacterial activity in direct contact for both of the tested bacterial strains after 24 h incubation (Figure S2a,c). Moreover, several bacterial colonies were observed directly under the standard samples in direct contact. All of the Petri dishes were densely populated by the bacterial colonies, except for very small areas around or under the samples made of hybrid DACHsilane fibres. The inhibition of bacteria for both strains was observed below the hybrid DACHsilane fibres (inset images Figure S2b,d) Moreover, the DACHsilane fibres showed a halo zone hint around the sample in the case of *S. aureus* (Figure S2b).

### 3.2.2. Assessment of Antibacterial Activity

The results related to the antibacterial activity in the solution were examined by calculating the bacterial cell growth reduction (CGR %) using Gram-positive bacteria *S. aureus* and Gram-negative bacteria *P. aeruginosa*. Figure 5 shows visible differences between the purely inorganic and hybrid DACHsilane fibres. The examined hybrid fibrous samples seemed to show significant antibacterial activity compared to the control and standard inorganic fibrous samples (Table S1, Figures S3–S5 in the Supplement). The antibacterial activity of the purely SiO<sub>2</sub> fibrous material was significantly less compared to the tested hybrid fibrous material. Better results were observed against *S. aureus* with 91% antibacterial activity than against *P. aeruginosa*, where the antibacterial activity reached only 87%. When we compare these results to the control for cell bacterial growth (Figure S3), the inhibition activity for both bacterial strains is even higher than 99.9%, which is in close agreement with the recent literature [25]. The results obtained from this experiment (Figure 5) closely correspond to the bacterial adhesion test mentioned below, where *P. aeruginosa* has a higher tendency to adhere to the surface of the hybrid fibrous sample compared to *S. aureus*.

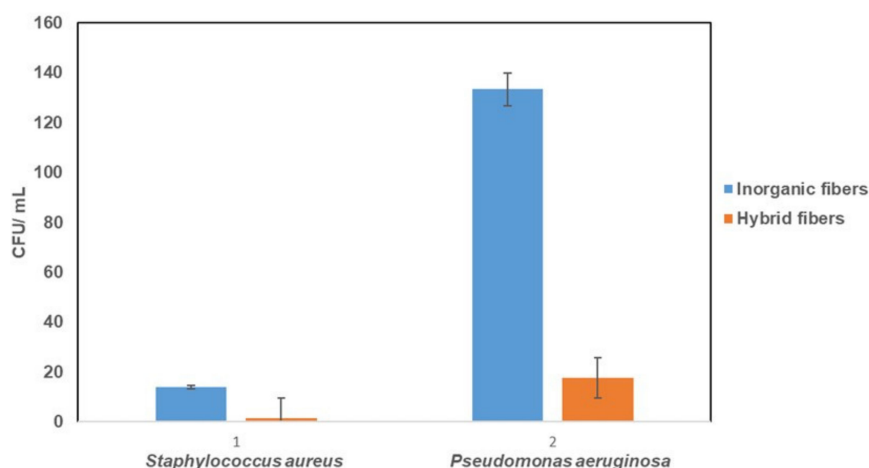


**Figure 5.** Comparison of the antibacterial activity for pure inorganic SiO<sub>2</sub> fibres and hybrid DACHsilane fibres against *S. aureus* and *P. aeruginosa*.

### 3.2.3. Bacterial Adhesion Activity

The bacterial adhesion to the surfaces of the fibrous samples against *S. aureus* and *P. aeruginosa*, was assessed by fluorescence imaging, see Figure 6. The green and red fluorescent spots indicate the live and dead bacteria, respectively. They were observed on the surface of the inorganic and hybrid fibres after 1 h incubation in the bacterial suspensions. The inorganic fibrous samples mostly exhibited green fluorescent spots scattered on the surface in both cases, suggesting live *S. aureus* and *P. aeruginosa* (Figure 6a,c). This fact indicates a lack of antibacterial properties of the tested standard SiO<sub>2</sub> fibres. Although the hybrid fibrous sample (DACHsilane) still shows a widespread attachment of both bacterial strains on its surface, it is important to note that most of them have a red fluorescence (Figure 6b,d), indicating a higher number of dead *S. aureus* and *P. aeruginosa* bacterial cells than viable (green) ones. Moreover, the bacterial adhesion to the surface of hybrid fibres is significantly weaker compared to the adhesion of the tested standard material for both bacterial strains. This observation is in agreement with the literature, where the antibacterial behaviour of similar molecule-based DACH derivatives was described [6]. The obtained results indicate that the activity of hybrid fibrous samples against *P. aeruginosa* is stronger in direct contact (Figure 6d).



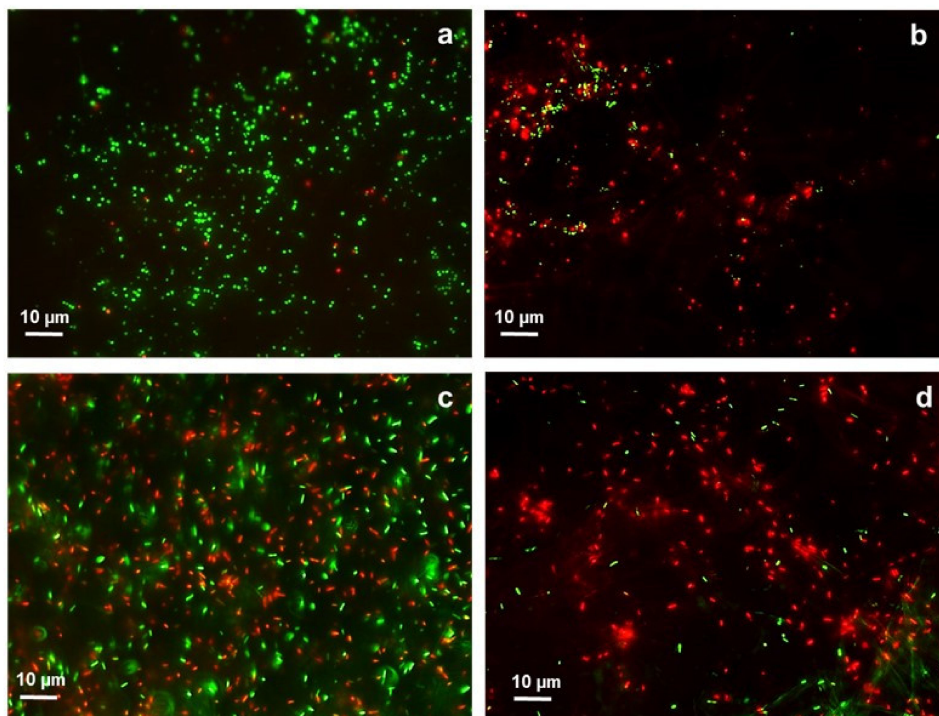


**Figure 6.** Fluorescence microscopy images of *S. aureus* on the surface of inorganic SiO<sub>2</sub> fibres (a) and on the surface of hybrid DACHsilane fibres (b). *P. aeruginosa* present on the surface of inorganic SiO<sub>2</sub> fibres (c) and on the surface of hybrid DACHsilane fibres (d). Green dots indicate live cells, while red dots dead cells.

### 3.3. Cytocompatibility Assessments

The cell viability assay performed on 3T3-A31 murine fibroblasts proved the cytocompatibility of the hybrid DACHsilane fibres in all three tested concentrations due to the viability highly exceeding the 70% CC level. As shown in Figure 7, exposure to the DACHsilane fibre extract led to increased cell viability in the case of the 500 μg/mL and 250 μg/mL extracts. The DACHsilane extracts had a concentration-dependent effect on cells as an increase in the extract concentration led to an increase in the cell viability from  $97.2 \pm 7.3\%$  (125 μg/mL) up to  $115.1 \pm 4.9\%$  (500 μg/mL). This led us to believe that the degradation products of the DACHsilane fibres are favouring cell proliferation. This effect was also observed with the inorganic silica dioxide nanofibres but in lower concentrations below 250 μg/mL (Figure 7). These findings were supported by a cell morphology analysis (see Figure S6 in the Supplement).

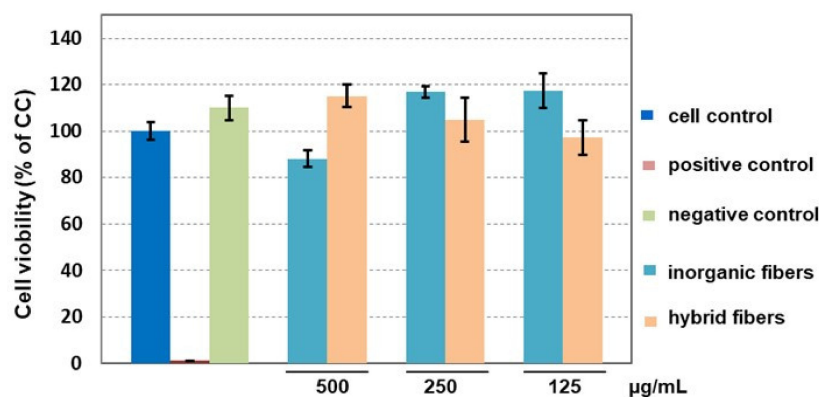


**Figure 7.** Comparison of the impact of hybrid DACHsilane nanofibres on the viability of 3T3-A31 cells compared to inorganic silica dioxide nanofibres as a control.

#### 4. Conclusions

Homogeneous, purely organosilane fibres consisting of a (1*S*,2*S*)-cyclohexane-1,2-diamine bis-silane derivative in combination with TEOS were prepared for the first time in a one-pot sol-gel synthesis and electrospinning. The spinnable organosilane solution was acquired starting from a suitable choice of sol-gel processing parameters without the aid of electrospinning polymeric or surfactant easers. The resulting hybrid organosilane fibrous mat was confirmed to be uniform, thermally stable up to 200 °C, and sufficiently elastic. The prepared hybrid fibrous samples showed very promising antibacterial activity, particularly in direct contact with both of the tested pathogenic bacterial strains *S. aureus* and *P. aeruginosa*. These findings indicate that the organosilane fibres on the basis of (1*S*,2*S*)-cyclohexane-1,2-diamine may be a promising tool in the framework of the global issue of drug resistance caused by pathogenic bacteria. The assumptions made are also supported by the cytocompatibility study proving their biocompatibility and positive impact on fibroblasts viability, which may lead to a positive impact on wound healing.

**Supplementary Materials:** The following are available online at <http://www.mdpi.com/2073-4360/12/1/206/s1>, Figure S1: Thermogravimetric analysis of the prepared hybrid DACHsilane fibers coupled with FTIR spectroscopy; Figure S2: Qualitative test describing the inhibition zones for standard sample—pure SiO<sub>2</sub> fibers a) and hybrid DACHsilane fibers b) against *S. aureus*; pure SiO<sub>2</sub> fibers c) and hybrid DACHsilane fibers d) against *P. aeruginosa*. Scale bar 1 cm; Figure S3: Control related to the bacterial cell growth of *Staphylococcus aureus* (S.A.) and *Pseudomonas aeruginosa* (P.A.). Both bacterial strains were diluted 100 times. Scale bar 1 cm; Figure S4: The bacterial cell growth of *Staphylococcus aureus* (S.A.) on the inorganic fiber sample a) and on the hybrid fiber sample b). Scale bar 1 cm; Figure S5: The bacterial cell growth of *Pseudomonas aeruginosa* (P.A.) on the inorganic fiber sample a) and on the hybrid fiber sample b). Scale bar 1 cm; Figure S6: The 3T3-A31 cells spindle-like morphology after 24 hours exposure to the DACHsilane fibres extracts (a) 0 µg/mL (CC), (b) 125 µg/mL, (c) 250 µg/mL and (d) 500 µg/mL Merge of modular contrast visualization and nucleus staining (DAPI) (Leica DMi8, obj. 20×). Scale bar 100 µm; Table S1: Antibacterial activity of the tested fibrous samples against *Staphylococcus aureus* and *Pseudomonas aeruginosa*.

**Author Contributions:** Conceptualization—V.M. and B.H.; methodology—J.H.; validation—J.H., M.Ř. and V.M.; formal analysis—J.B. and D.T.; investigation—B.H., V.M., D.T. and M.R.; resources—J.H. and M.Ř.; data curation—J.B.; writing—original draft preparation—V.M. and B.H.; writing—review and editing—M.Ř. and J.H.; visualization—V.M., B.H., M.R., J.B., M.Ř.; supervision—J.H. All authors have read and agreed to the published version of the manuscript.

**Funding:** This research was funded by the Project 18-09824S of the Czech Science Foundation (GA CR) and by the Ministry of Education, Youth and Sports of the Czech Republic, specific university research (MSMT No. 21-SVV/2019) and the European Union—European Structural and Investment Funds in the framework of the Operational Programme Research, Development, and Education project “Hybrid Materials for Hierarchical Structures (HyHi)”, Reg. No. CZ.02.1.01/0.0/0.0/16\_019/0000843.

**Conflicts of Interest:** The authors declare no conflict of interest.

#### References

1. Bogdanović, U.; Dimitrijević, S.; Škapin, S.D.; Popović, M.; Rakočević, Z.; Leskovic, A.; Petrović, S.; Stoiljković, M.; Vodnik, V. Copper-polyaniline nanocomposite: Role of physicochemical properties on the antimicrobial activity and genotoxicity evaluation. *Mater. Sci. Eng. C* **2018**, *93*, 49–60. [[CrossRef](#)] [[PubMed](#)]
2. Nazir, A.; Kadri, S.M. An overview of hospital acquired infections and the role of the microbiology laboratory. *Int. J. Res. Med. Sci.* **2017**, *2*, 21–27. [[CrossRef](#)]
3. Khan, H.A.; Baig, F.K.; Mehboob, R. Nosocomial infections: Epidemiology, prevention, control and surveillance. *Asian Pac. J. Trop. Biomed.* **2017**, *7*, 478–482. [[CrossRef](#)]
4. Wang, Y.; Han, B.; Xie, Y.; Wang, H.; Wang, R.; Xia, W.; Li, H.; Sun, H. Combination of gallium(III) with acetate for combating antibiotic resistant *Pseudomonas aeruginosa*. *Chem. Sci.* **2019**, *10*, 6099–6106. [[CrossRef](#)] [[PubMed](#)]
5. Lichter, J.A.; Van Vliet, K.J.; Rubner, M.F. Design of Antibacterial Surfaces and Interfaces: Polyelectrolyte Multilayers as a Multifunctional Platform. *Macromolecules* **2009**, *42*, 8573–8586. [[CrossRef](#)]

6. Sharma, M.; Joshi, P.; Kumar, N.; Joshi, S.; Rohilla, R.K.; Roy, N.; Rawat, D.S. Synthesis, antimicrobial activity and structure–activity relationship study of N,N-dibenzyl-cyclohexane-1,2-diamine derivatives. *Eur. J. Med. Chem.* **2011**, *46*, 480–487. [[CrossRef](#)] [[PubMed](#)]
7. Beena, J.S.; Kumar, N.; Kidwai, S.; Singh, R.; Rawat, D.S. Synthesis and antitubercular activity evaluation of novel unsymmetrical cyclohexane-1,2-diamine derivatives. *Arch. Pharm. Weinh.* **2012**, *345*, 896–901. [[CrossRef](#)]
8. Beena, J.S.; Kumar, D.; Kumbukgolla, W.; Jayaweera, S.; Bailey, M.; Alling, T.; Ollinger, J.; Parish, T.; Rawat, D.S. Antibacterial activity of adamantyl substituted cyclohexane diamine derivatives against methicillin resistant *Staphylococcus aureus* and *Mycobacterium tuberculosis*. *RSC Adv.* **2014**, *4*, 11962–11966. [[CrossRef](#)]
9. Kumar, D.; Raj, K.K.; Bailey, M.; Alling, T.; Parish, T.; Rawat, D.S. Antimycobacterial activity evaluation, time-kill kinetic and 3D-QSAR study of C-(3-aminomethyl-cyclohexyl)-methylamine derivatives. *Bioorg. Med. Chem. Lett.* **2013**, *23*, 1365–1369. [[CrossRef](#)]
10. KICKELBICK, G. (Ed.) *Hybrid Materials: Synthesis, Characterization, and Applications*; Wiley-VCH: Weinheim, Germany, 2007.
11. Gómez-Romero, P.; Sanchez, C. (Eds.) *Functional Hybrid Materials*; Wiley-VCH: Weinheim, Germany, 2004.
12. Sanchez, C.; Belleville, P.; Popall, M.; Nicole, L. Applications of advanced hybrid organic–inorganic nanomaterials: From laboratory to market. *Chem. Soc. Rev.* **2011**, *40*, 696. [[CrossRef](#)]
13. Faustini, M.; Nicole, L.; Ruiz-Hitzky, E.; Sanchez, C. History of Organic-Inorganic Hybrid Materials: Prehistory, Art, Science, and Advanced Applications. *Adv. Funct. Mater.* **2018**, *28*, 1704158. [[CrossRef](#)]
14. Sanchez, C.; Julián, B.; Belleville, P.; Popall, M. Applications of hybrid organic–inorganic nanocomposites. *J. Mater. Chem.* **2005**, *15*, 3559–3592. [[CrossRef](#)]
15. Gugliemli, M.; Kickelbick, K.; Martucci, A. (Eds.) *Advances in Sol-Gel Derived Materials and Technologies. In Sol-Gel Nanocomposites*; Springer: New York, NY, USA, 2013.
16. Kaur, S.; Gallei, M.; Ionescu, E. Polymer–Ceramic Nanohybrid Materials. In *Organic-Inorganic Hybrid Nanomaterials*; Kalia, S., Haldorai, Y., Eds.; Springer International Publishing: Cham, Switzerland, 2014; Volume 267, pp. 143–185.
17. Rai, R.V.; Bai, J.A. *Nanoparticles and Their Potential Application as Antimicrobials, Science against Microbial Pathogens: Communicating Current Research and Technological Advances*; Méndez-Vilas, A., Ed.; Formatex, Microbiology Series: Badajoz, Spain, 2011; Volume 1, pp. 197–209.
18. Ciraldo, F.E.; Schnepf, K.; Goldmann, W.H.; Boccaccini, A.R. Development and Characterization of Bioactive Glass Containing Composite Coatings with Ion Releasing Function for Antibiotic-Free Antibacterial Surgical Sutures. *Materials* **2019**, *12*, 423. [[CrossRef](#)] [[PubMed](#)]
19. Tao, S.; Li, G.; Yin, J. Fluorescent nanofibrous membranes for trace detection of TNT vapor. *J. Mater. Chem.* **2007**, *17*, 2730. [[CrossRef](#)]
20. Schramm, C.; Rinderer, B.; Tessadri, R. Synthesis and characterization of novel ultrathin polyimide fibres via sol-gel process and electrospinning. *J. Appl. Polym. Sci.* **2013**, *128*, 1274–1281. [[CrossRef](#)]
21. Gualandi, C.; Celli, A.; Zucchelli, A.; Focarete, M.L. Nanohybrid Materials by Electrospinning. In *Organic-Inorganic Hybrid Nanomaterials*; Kalia, S., Haldorai, Y., Eds.; Springer International Publishing: Cham, Switzerland, 2014; Volume 267, pp. 87–142.
22. Darder, M.; Aranda, P.; Ruiz-Hitzky, E. Bionanocomposites: A New Concept of Ecological, Bioinspired, and Functional Hybrid Materials. *Adv. Mater.* **2007**, *19*, 1309–1319. [[CrossRef](#)]
23. Ding, Y.; Li, W.; Correia, A.; Yang, Y.; Zheng, K.; Liu, D.; Schubert, D.W.; Boccaccini, A.R.; Santos, H.A.; Roether, J.A. Electrospun Polyhydroxybutyrate/Poly( $\epsilon$ -caprolactone)/Sol-Gel-Derived Silica Hybrid Scaffolds with Drug Releasing Function for Bone Tissue Engineering Applications. *ACS Appl Mater Interfaces* **2018**, *10*, 14540–14548. [[CrossRef](#)]
24. Ding, Y.; Yao, Q.; Li, W.; Schubert, D.W.; Boccaccini, A.R.; Roether, J.A. The evaluation of physical properties and in vitro cell behavior of PHB/PCL/sol–gel derived silica hybrid scaffolds and PHB/PCL/fumed silica composite scaffolds. *Colloids Surf. B Biointerfaces* **2015**, *136*, 93–98. [[CrossRef](#)]
25. Dhand, C.; Balakrishnan, Y.; Ong, S.T.; Dwivedi, N.; Venugopal, J.R.; Harini, S.; Leung, C.M.; Low, K.Z.W.; Loh, X.J.; Beuerman, R.W.; et al. Antimicrobial quaternary ammonium organosilane cross-linked nanofibrous collagen scaffolds for tissue engineering. *Int. J. Nanomed.* **2018**, *13*, 4473–4492. [[CrossRef](#)]
26. Moreau, J.J.E.; Vellutini, L.; Wong Chi Man, M.; Bied, C. Shape-Controlled Bridged Silsesquioxanes: Hollow Tubes and Spheres. *Chem. Eur. J.* **2003**, *9*, 1594–1599. [[CrossRef](#)]

27. Iimura, K.; Oi, T.; Suzuki, M.; Hirota, M. Preparation of silica fibres and non-woven cloth by electrospinning. *Adv. Powder Technol.* **2010**, *21*, 64–68. [[CrossRef](#)]
28. Brus, J.; Urbanová, M.; Strachota, A. Epoxy Networks Reinforced with Polyhedral Oligomeric Silsesquioxanes: Structure and Segmental Dynamics as Studied by Solid-State NMR. *Macromolecules* **2008**, *41*, 372–386. [[CrossRef](#)]
29. Liu, Z.; Qi, L.; An, X.; Liu, C.; Hu, Y. Surface Engineering of Thin Film Composite Polyamide Membranes with Silver Nanoparticles through Layer-by-Layer Interfacial Polymerization for Antibacterial Properties. *ACS Appl. Mater. Interfaces* **2017**, *9*, 40987–40997. [[CrossRef](#)] [[PubMed](#)]
30. KICKELBICK, G. Introduction to Hybrid Materials. In *Hybrid Materials*; John Wiley & Sons, Ltd.: Hoboken, NJ, USA, 2007; pp. 1–48.
31. Brinker, C.J.; Scherer, G. *Sol-Gel Science: The Physics and Chemistry of Sol-Gel Processing*; Elsevier Inc.: Amsterdam, The Netherlands, 2013.
32. Sakka, S.; Kamiya, K. The sol-gel transition in the hydrolysis of metal alkoxides in relation to the formation of glass fibres and films. *J. Non-Cryst. Solids* **1982**, *48*, 31–46. [[CrossRef](#)]
33. Liu, F.; Fu, L.; Wang, J.; Meng, Q.; Li, H.; Guo, J.; Zhang, H. Luminescent film with terbium-complex-bridged polysilsesquioxanes. Electronic supplementary information (ESI) available: IR, UV-Vis and excitation spectra and decay curves. *New J. Chem.* **2003**, *27*, 233–235. [[CrossRef](#)]
34. Liu, N.; Yu, K.; Smarsly, B.; Dunphy, D.R.; Jiang, Y.-B.; Brinker, C.J. Self-Directed Assembly of Photoactive Hybrid Silicates Derived from an Azobenzene-Bridged Silsesquioxane. *J. Am. Chem. Soc.* **2002**, *124*, 14540–14541. [[CrossRef](#)] [[PubMed](#)]
35. Álvaro, M.; Benitez, M.; Das, D.; Ferrer, B.; García, H. Synthesis of Chiral Periodic Mesoporous Silicas (ChiMO) of MCM-41 Type with Binaphthyl and Cyclohexadiyl Groups Incorporated in the Framework and Direct Measurement of Their Optical Activity. *Chem. Mater.* **2004**, *16*, 2222–2228. [[CrossRef](#)]
36. Innocenzi, P. Infrared spectroscopy of sol-gel derived silica-based films: A spectra-microstructure overview. *J. Non-Cryst. Solids* **2003**, *316*, 309–319. [[CrossRef](#)]
37. Olejniczak, Z.; Łęczka, M.; Cholewa-Kowalska, K.; Wojtach, K.; Rokita, M.; Mozgawa, W. <sup>29</sup>Si MAS NMR and FTIR study of inorganic-organic hybrid gels. *J. Mol. Struct.* **2005**, *744–747*, 465–471. [[CrossRef](#)]



© 2020 by the authors. Licensee MDPI, Basel, Switzerland. This article is an open access article distributed under the terms and conditions of the Creative Commons Attribution (CC BY) license (<http://creativecommons.org/licenses/by/4.0/>).